Bidirectional reflectance study on dry, wet, and submerged particulate layers: effects of pore liquid refractive index and translucent particle concentrations

Hao Zhang and Kenneth J. Voss

We performed extensive bidirectional reflectance measurements on dry, wet, and submerged particulate layers with various albedos to investigate the darkening effect caused by wetting with fluids. It was found that, in addition to the reduction of the refractive index contrast when there is a pore liquid (wetted), the concentration of translucent grains in a particulate layer and the surface roughness conditions of the individual grains make important contributions to the wetting-induced darkening effect. Reflectance measurements on glass–sediment mixtures confirmed that, as the concentration of translucent particles increases, the reflectance of the dry layers increases while that of the wetted layers decreases. Measurements indicate that neither the prediction made by the theory of Twomey *et al*. [Appl. Opt. **25,** 431 (1986)] nor that of Lekner and Dorf [Appl. Opt. **27,** 1278 (1988)] is sufficient.

OCIS codes: 010.4450, 280.0280, 120.5700, 290.4210, 030.5620.

1. Introduction

It is well known that many rough and absorbing surfaces look darker when wetted by water.[1] A thorough understanding of the underlying mechanism of this familiar phenomenon has applications in remote sensing and other related fields.[2–4] Twomey *et al*.[2] (TBM) formulated a theory to predict the effect of wetting on the albedo and reflectance based on the isotropic multiple-scattering approximation. They attributed the darkening effect to an increase in forward scattering by the particulates owing to a decrease in the refractive index contrast between the particles and the medium. This decrease allows light to penetrate farther into the sediment and increases the probability that the light will be absorbed before exiting the sediment. Lekner and Dorf[5] (LD) proposed a competing theory based on Angstrom's geometrical optics model.[6] For this approach diffuse reflectance from a rough surface will be reflected at the air–liquid interface, and less light will escape. Both the TBM and the LD models could qualitatively explain the darkening of sand and soil. However, the limited available albedo data and the lack of bidirectional reflectance distribution function (BRDF) data did not allow a convincing separation of these two effects. In recent years, we have made extensive BRDF measurements on various types of sediment particle, both dry and submerged.[7,8] In our work investigating predictive and invertible models of natural benthic sediments it is important to understand the effect of interstitial water on the BRDF. In this work we present BRDF measurements on dry, wet, and submerged particulate layers with varied optical properties. The albedos calculated from our BRDF data are compared with model predictions to determine the mechanisms responsible for the darkening effect.

2. Experimental Method

The BRDF data were taken with our BRDF meter, which has been described in greater detail elsewhere.[9] Briefly, three colors of incident light (red at 657 nm, green at 570 nm, and blue at 475 nm) can be directed to the sample surface at zenith angles of 0°, 5°, 15°, 25°, 35°, 45°, 55°, and 65°. The reflected light is simultaneously measured at 107 viewing directions with zenith angles from 5° to 65° and azimuth angles from ±5° to ±170°. This instrument was designed to measure submerged benthic sediment *in situ*; however, we can also take measurements of dry and wetted particulate layers. We present the

The authors are with the Department of Physics, University of Miami, 1320 Campo Sano Drive, Coral Gables, Florida 33146. K. J. Voss's e-mail address is voss@physics.miami.edu.

Received 19 May 2006; revised 4 August 2006; accepted 9 August 2006; posted 11 August 2006 (Doc. ID 71165).

0003-6935/06/348753-11$15.00/0

BRDF data in terms of the reflectance factor (REFF),[10] which is conveniently compared with a perfect Lambertian surface. The REFF is the ratio of the bidirectional reflectance of the sample r_S to that of a perfect Lambertian diffuser r_L, i.e.,

$$\mathrm{REFF}(\theta_i,\ \phi_i;\ \theta_v,\ \phi_v) = \frac{r_S(\theta_i,\ \phi_i;\ \theta_v,\ \phi_v)}{r_L(\theta_i)},$$

where θ_i and θ_v are the incident and viewing zeniths, ϕ_i and ϕ_v are the incident and viewing azimuth angles, respectively; $r_S(\theta_i, \phi_i; \theta_v, \phi_v)$ is defined as the ratio of the radiance reflected by the surface in a given direction, $L_r(\theta_v, \phi_v)$ to the collimated irradiance incident on the surface, $E_i(\theta_i, \phi_i)$:

$$r_S(\theta_i,\ \phi_i;\ \theta_v,\ \phi_v) = \frac{L_r(\theta_v,\ \phi_v)}{E_i(\theta_i,\ \phi_i)}.$$

r_L is the bidirectional reflectance of a perfect Lambertian diffuser

$$r_L = \frac{\mu_0}{\pi},$$

where μ_0 is $\cos\theta_i$. With the above definitions, the REFF is

$$\mathrm{REFF}(\theta_i,\ \phi_i;\ \theta_v,\ \phi_v) = \frac{\pi r_S(\theta_i,\ \phi_i;\ \theta_v,\ \phi_v)}{\mu_0}.$$

We assume that the surfaces are azimuthally symmetric such that the REFF depends not on ϕ_i and ϕ_v, but on $\phi_i - \phi_v = \phi$. Then bidirectional quantities defined above may also be expressed in terms of phase angle g defined by

$$g = \cos^{-1}[\cos\theta_i \cos\theta_v + \sin\theta_i \sin\theta_v \cos(\phi_v - \phi_i)],$$

with $g = 0$ corresponding to the exact backscattering direction and large g ($g > 90°$) the forward-scattering direction. The REFF will be displayed against g throughout this work. Positive phase angles correspond to $0° \le \phi \le 180°$, and the negative phase angles correspond to $180° \le \phi \le 360°$. For a perfect surface, the REFF at positive and negative phase angles should be the same; however, for real surfaces, differentiating between the two sides allows us to show how well we made the surface. Asymmetries would point to problems with the surface geometry. Note that since we are looking at reflected light, we are restricted to $\theta_v < 90°$. If θ_i is zero, $g = \theta_v$, and is less than 90°, if θ_i is greater than zero, larger g values can be measured.

The directional albedo at each incident angle θ_i can be evaluated by

$$\alpha(\theta_i) = \pi^{-1}\int_{2\pi}\int_{\pi/2} \mathrm{REFF}(\theta_v,\ \phi_v)\cos\theta_v \sin\theta_v d\theta_v d\phi_v$$

from the measured viewing REFF.[8] We limit our discussions to red incident light for two reasons: (1) most particulate samples we have measured in past years show a very weak, or no, color dependence in the visible range; and (2) the red REFF has the highest signal-to-noise ratio among the three colors in the BRDF meter.

Field samples collected for this work were rinsed and then bleached with 6% sodium hypochlorite for 24 h to remove organic matter. Most of the samples were sieved into different size distributions. For the dry samples, the sample was slowly poured into a 1 cm deep polyvinyl chloride (PVC) sample holder. The holder was tapped from the side to settle the sediment until the sediment stabilized, and the surface was then smoothed with a straight edge. Four rotations of the samples were measured with the BRDF meter to minimize any remaining surface orientation bias. Due to the stochastic nature of such particulate layers, we have typically found a 1%–2% albedo variation between replicate samples because of different surface layer realizations. After measuring the dry sample, water was slowly applied to the sand surface with an eyedropper. The wetting process was started from the edge of the surface to minimize any surface morphology modifications during the wetting process. Water was added until the air bubbles stopped coming out of the surface and the sample appeared over saturated. The extra water on the surface was blotted by a soft paper to remove all liquid puddles. We have found that any extra water left on the surface caused a strong specular peak especially at large illumination zenith angles. When doing the submerged measurement, great care was taken to preserve the flat surface underwater. The surface quality was checked both before and after the measurement to ensure that the unavoidable water flow, caused by putting the BRDF meter down on the sample, did not disturb the surface. The calibration of the BRDF meter is described elsewhere,[9] but in essence it was done with comparison to a Spectralon plaque (Labsphere).[11]

3. Results

A. Shallow Water Benthic Sediments

We started with three typical shallow water sediments collected near Lee Stocking Island, Exumas, Bahamas, during Summer 2000. The first sample was an ooid sand with smooth, round grains, a lustrous surface, and diameters between 0.25 and 0.5 mm (*Sample A*). The second sample was mainly broken shells with a size distribution between 0.125 and 0.25 mm (*Sample G*). The third sample was composed of large (1–2 mm) and rough platelets (*Rough*). These samples were chosen because they represented a variety of the samples measured to date. For example, *Sample G* had the highest albedo values, and *Rough* had the strongest backscattering peak (hotspot) of all the samples.

Figure 1 shows the dry and water-wetted REFF of these three samples at normal and 65° incidence. The

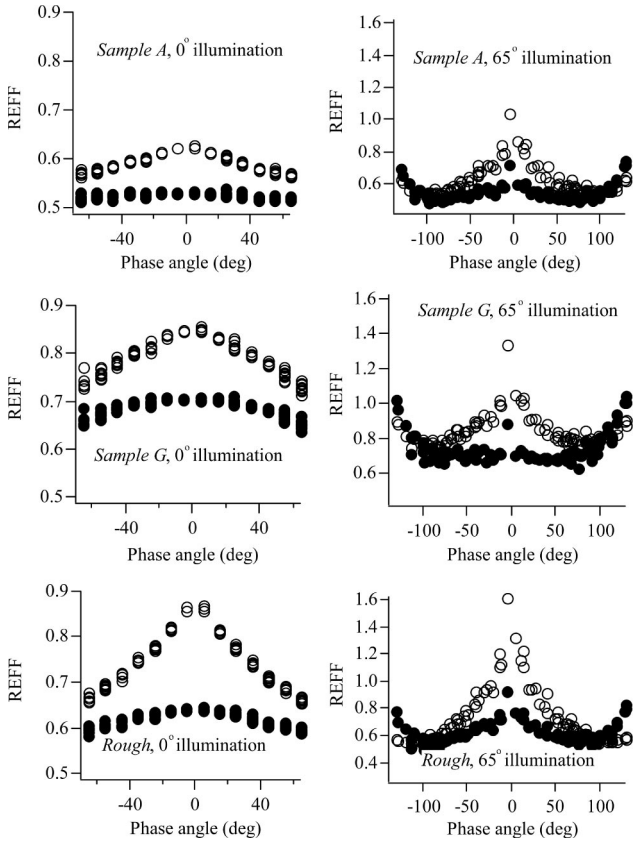

Fig. 1. Three dry and water wetted typical benthic sediment samples. Open circles are dry and solid circles are water wetted.

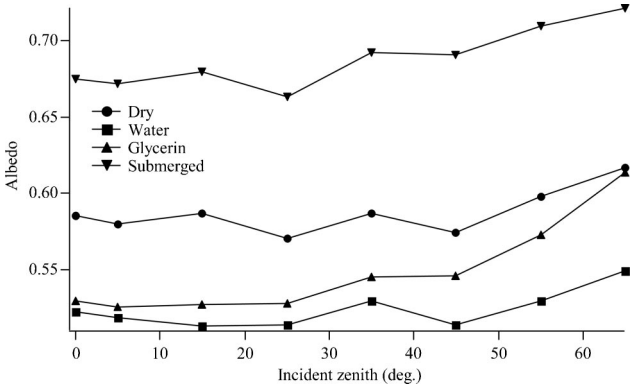

Fig. 2. Albedos of dry, submerged, water, and glycerin wetted *Sample A* at eight illumination angles.

REFF versus the positive and negative phase angles (as defined in Section 2) demonstrates that the angular data are indeed azimuthally symmetric. Also note that at 65° incidence the phase angle range is larger than normal incidence, as discussed earlier. Beginning with the dry measurements, we can see from Fig. 1 that at normal illumination *Sample A* is the most Lambertian while *Rough* is the most anisotropic among the three. At 65° illumination, both *Sample A* and *Sample G* developed a forward-scattering peak in addition to the hotspot, while *Rough* has only a strong and broad hotspot. At normal incidence, the effect of wetting is to reduce the overall reflectance and make the surface more Lambertian than when dry; all three samples have small variations ranging from 3% (*Sample A*) to 7% (*Rough*) for phase angles from 0° to 65°. At 65° incidence, the wetting decreases the backscattering peak but relatively increases the forward-scattering peak ($g > 90°$). Even for *Rough* the forward-scattering peak becomes larger than the hotspot. The angular dependence of the REFF on wetting follows, qualitatively, the idea of TBM, adding the wetting fluid increased the forward scattering and decreased the backscattering.

Although wetting with water caused significant changes in the measured REFF as shown above, visually these three samples are not appreciably darker when wet than when dry, especially *Sample A*. This is in contrast to our daily experience that many sand or soil layers appear darker when wet.

According to TBM, increasing the fluid refractive index should decrease the reflectance. However, for *Sample A*, a glycerin ($n = 1.47$) wetted layer did not appear significantly darker to the naked eye. In Fig. 2 we show *Sample A*'s dry, submerged, water wetted, and glycerin wetted directional albedos at eight illumination angles (we will discuss the submerged measurement in Subsection 3.D). Note that wetting with water or glycerin decreases the albedo only by approximately 10%. The slightly higher albedo values of the glycerin wetted layer were caused by the specular reflectance produced by residual glycerin on the layer surface because of its viscid nature. According to TBM, surfaces with either very high or very low albedos will have little wetting effect. However, *Sample A* has a dry albedo value of 0.6, and hence is expected to have a more appreciable wetting effect. The lack of an appreciable wetting effect led us to look for other samples with stronger wetting effects. These samples are described below in Subsection 3.B.

B. Beach Sands, Soil Particles, and *Glass*

We collected four additional samples from different sites: volcanic black beach sand from the Big Island, Hawaii (*Volcanic*), sand from the beach at Crandon Park, Miami (*Crandon*); sand from the beach at the University of Miami's Rosential School of Marine and Atmosphere Science (*RSMAS*), and soil particles from the University of Miami's Gifford Arboretum (*Soil*). In addition, we measured black silica sand used as cigarette-urn sand at the University of Miami (*Black Sand*) and nonabsorbing broken glass obtained by crushing microscope glass slides (*Glass*) (Fisher brand, catalog number 12-550C). These six samples run the gamut of albedo from nearly 0 (totally absorbing) to approximately 0.7 (weakly absorbing). For *Crandon*, *RSMAS* and *Soil* particles, sieved grains with a size distribution of 0.25–0.5 mm in diameter were used. For the *Volcanic* and *Black Sand* the size selection was between 0.5 and 1 mm because this was the dominant size. For *Glass* the grains were passed through a 1 mm mesh sieve, as this was the

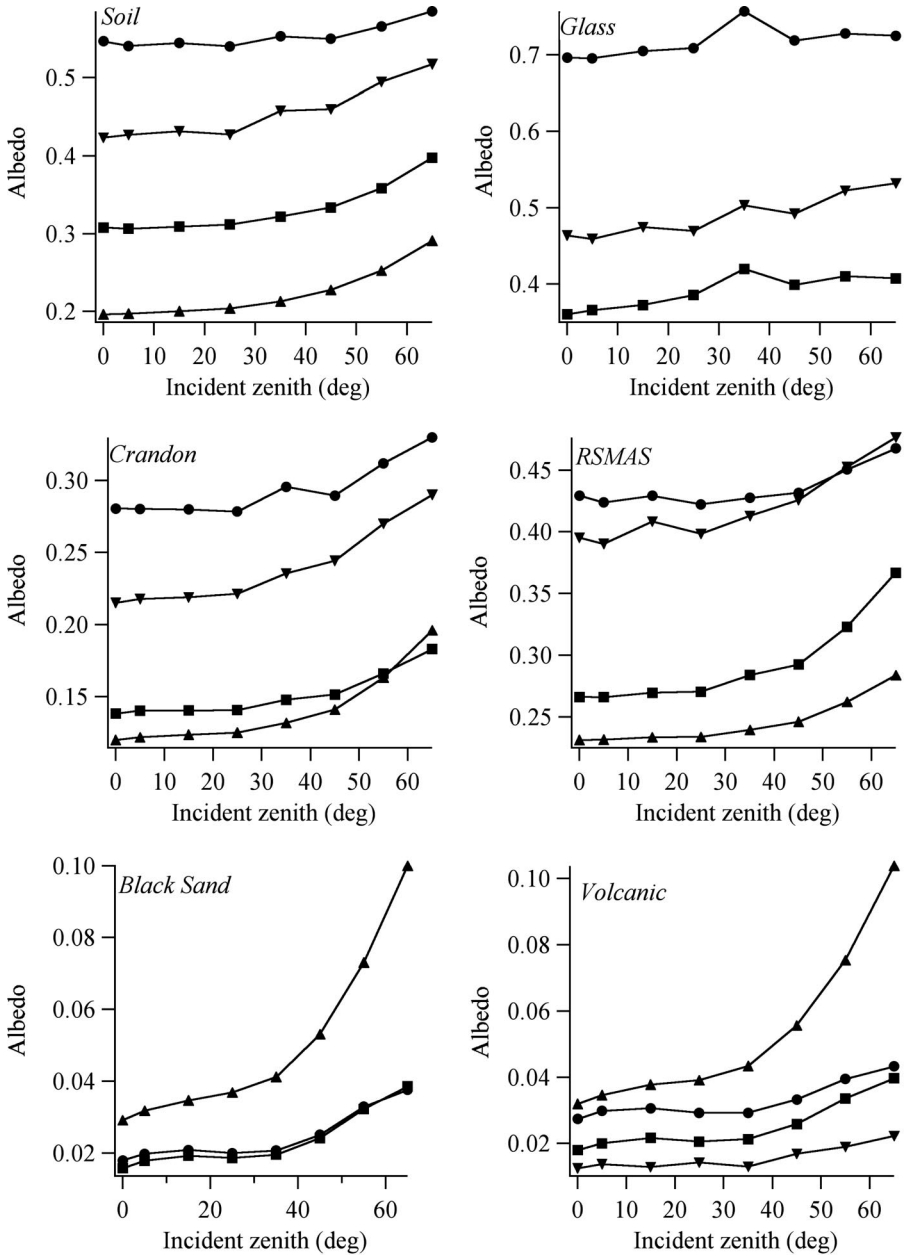

Fig. 3. Six sediment samples: dry, submerged, water, and glycerin wetted, symbols as in Fig. 2. For *Black Sand* the submerged albedo is not shown.

end member of the *Sample A–Glass* mixture described in Subsection 3.C.

Figure 3 displays dry, submerged, water, and glycerin wetted albedos for all six samples described above (again, we will defer the discussion on submerged measurements until Subsection 3.D). It should be noted that for *Glass*, a 4 cm deep black PVC holder was used in measurements. As an extra test, a piece of white paper was placed on the bottom of the holder to test that the layers were thick enough for BRDF measurement. The results indicated that for dry and water wetted layers the difference in the measured BRDF and albedo introduced by placing a white paper on the bottom, versus no paper and the original black holder, were within measurement uncertainties, and thus this holder could be considered optically deep. However, when glycerin was used as a wetting liquid, a difference was seen in the wetted layer when the white paper was added, thus 4 cm is not optically deep. For this reason, the glycerin wetted albedos for the *Glass* are not shown. All other samples were tested and found to be sufficiently thick to be considered optically deep.

It is seen that, except for the two very dark samples (*Volcanic* and *Black Sand*), all these samples are significantly darker when wetted with water. When we inspected the natural samples with a stereomicroscope we discovered that many of the grains were translucent quartz particles. An estimate of the fraction of translucent (as opposed to opaque) particles was made

from stereomicroscope images. In going from dry to water wetted, *Glass* which contained 100% translucent grains, exhibited the greatest reduction in albedo, followed by *Crandon* (36% translucent particles), *RSMAS* (50% translucent particles), and *Soil* (80% translucent particles) at normal incidence. We also saw that for these three samples the glycerin wetted layer was significantly darker than the water wetted one. In this work, "translucent" particles simply stand for quartzlike particles with a low absorption coefficient (small imaginary refractive index) and/or low internal scattering. For these particles, a large portion of the light incident on the grains is transmitted.

For the darker samples we saw that, at normal incidence, water wetting decreased the dry albedos by 35% for the *Volcanic* but there was practically no effect for the *Black Sand*. If one looks at the stereomicroscope images of these two samples, it is evident that the *Volcanic* grains have more surface roughness and reflect light more diffusely. The *Black Sand* has a shiny surface. If one looks at the REFF of these two samples, the REFF of the *Black Sand* had very little change on wetting, while the *Volcanic* obviously decreased backscattering and increased (relatively) forward scattering when wetted. The difference in the wetting effect between the *Volcanic* and the *Black Sand* must be attributable to the change in scattering of the individual grains. The major physical difference between the two samples is the surface roughness of the individual particles.

The surface roughness of individual particles probably affects the albedo of the individual particles in a way similar to that LD predicted for the total surface, particularly for the particles on the surface of the layer. Light scattered from the surface of a particle with a rough surface is scattered more diffusely than for a particle with a smooth surface. If this surface is coated with water, then light will interact with a water–air surface when leaving the particle. For the diffusely scattering rough surface, more of this light hits the water–air surface at larger angles, and hence is reflected back to interact with the particle again and perhaps be absorbed. Thus the particles with a rough surface can appear darker, depending on the albedo of the surface of the individual particles.

The surfaces of the opaque grains found in these samples are not as smooth as *Sample A*. In addition, as mentioned, these samples contain translucent particles with varying concentrations. These two features must account for the larger decrease in reflectance when wetted. In an attempt to quantify the effects due to translucent particle concentration, we carried out BRDF measurements on mixtures of *Glass* and *Sample A*.

C. Mixtures of *Glass* and Ooid Sand

We dispersed *Glass* in *Sample A* with varied volume concentrations. The *Glass* used in the mixtures were sieved through a 1 mm mesh sieve. Figure 4 shows the REFF at normal and at 65° incident angles, for both dry and wet mixtures. The progressions from pure *Sample A* to pure *Glass* are opposite for dry and wet mixtures. For the dry samples, increasing the *Glass* concentration increases the REFF especially in the forward-scattering direction ($g > 90°$ at 65° incidence). However, for the wet mixtures, increasing the *Glass* concentrations decreases the REFF. This can be better demonstrated by plotting the albedo variation versus the *Glass* concentration, as shown in Fig. 5. For clarity, only normal and 65° incidence of the dry and water wetted albedos are displayed in Fig. 5. One can clearly see that increasing the glass concentrations can indeed lead to an enhanced darkening effect for the water wetted mixture. For wet samples, a clear decrease in the albedo from pure *Sample A* to pure *Glass* occurs at the two illumination angles. In the dry case, for concentrations of *Glass* $< 50\%$, the albedo does not change significantly. Above 50% the albedo clearly increases. Thus the difference between the wet and the dry albedos clearly increases with increasing translucent particle concentration.

To quantify the effect of mixing the translucent particles we applied two mixing formulas[10] to predict the dry and wet albedos of *Sample A–Glass* mixtures. The first one is the areal mixture formula, which is simply the linear sum of the reflectance of each component:

$$\alpha^{\mathrm{AM}} = F_1\alpha_1 + F_2\alpha_2, \tag{1}$$

where F_i and α_i are the area fraction (%) and the albedo of the individual species, respectively.

The second approach is the intimate mixture formula that is applied to single scattering quantities:

$$\varpi = \frac{\varpi_1 + \varepsilon\varpi_2}{1 + \varepsilon}, \tag{2}$$

where ϖ and ϖ_j are the single-scattering albedos of the mixture and the jth type particle, respectively, and the ratio ε is given by

$$\varepsilon = \frac{N_2\sigma_2}{N_1\sigma_1}, \tag{3}$$

for particles much larger than the wavelength, where N_j is the number density and σ_j is the geometric cross section of the jth type particle, respectively. For simplicity, the ratio ε is approximated by

$$\varepsilon \approx \frac{1 - \mathrm{glass}\%}{\mathrm{glass}\%},$$

where glass% is the percent volume of *Glass* in the sample. Next, the scaled single scattering albedo ϖ^* is given by the similarity relationship

$$\varpi^* = \frac{1 - \xi}{1 - \xi\varpi}\,\varpi, \tag{4}$$

where ξ is the asymmetry parameter of the mixture[10]

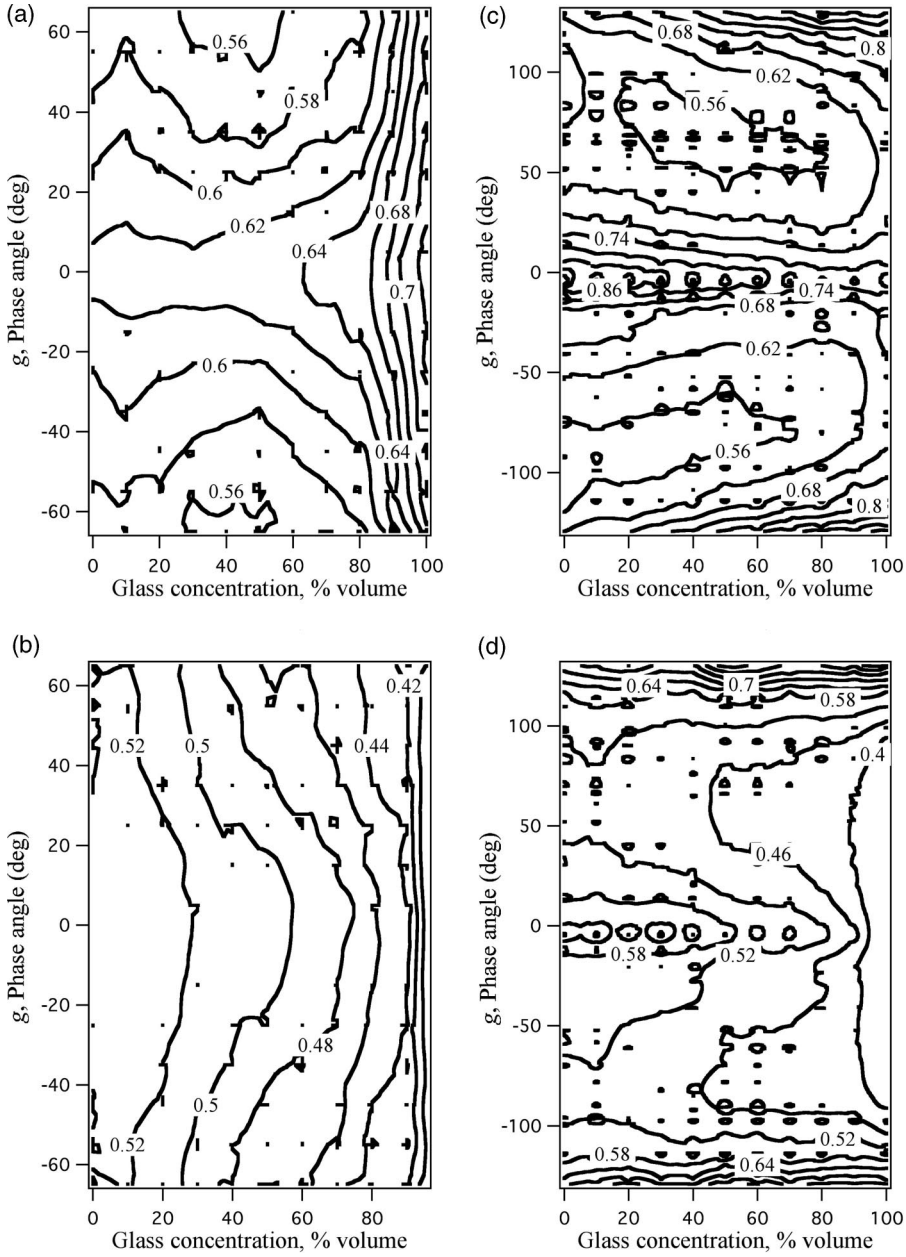

Fig. 4. REFF versus the *Glass* concentration and g phase angle: (a) normal incidence, dry; (b) normal incidence, wet; (c) 65° incidence, dry; (d) 65° incidence, wet.

$$\xi = \frac{(\varpi - \varpi_2)\varpi_1\xi_1 - (\varpi - \varpi_1)\varpi_2\xi_2}{(\varpi_1 - \varpi_2)\varpi}, \tag{5}$$

where ξ_j is the asymmetry parameter of the jth type particles. Finally, the diffuse reflectance r_o of the mixture is approximated by the albedo at the 60° zenith angle, and r_o is related to the scaled single scattering albedo by[10]

$$\alpha(60°) \approx r_0 = \frac{1 - \sqrt{1 - \varpi^*}}{1 + \sqrt{1 - \varpi^*}}. \tag{6}$$

To apply the mixing formula Eq. (5) to a binary mixture, the values of the asymmetry parameters of the two end members are needed. Vera *et al.*[12] measured the diffuse reflectance of small glass frits (~0.05 mm) and obtained an asymmetry parameter value of 0.9 by fitting data to their diffusion reflectance model. For the large glass frits used in this work, it is likely ξ has a slightly higher value, which we estimate to be 0.93. A similar ξ value has been used on highly forward-scattering snow grains.[13] For pure *Sample A*, we use a ξ value of 0.7. This is roughly the asymmetry parameter of a large ellipsoid with an aspect ratio of approximately 2 obtained by performing ray-tracing calculations.[14] When wetted, the ξ values for pure *Sample A* and *Glass* are estimated to be 0.9 and 0.96, respectively. Using Eq. (4), one obtains the following single-scattering albedo values for *Sample A*: 0.981

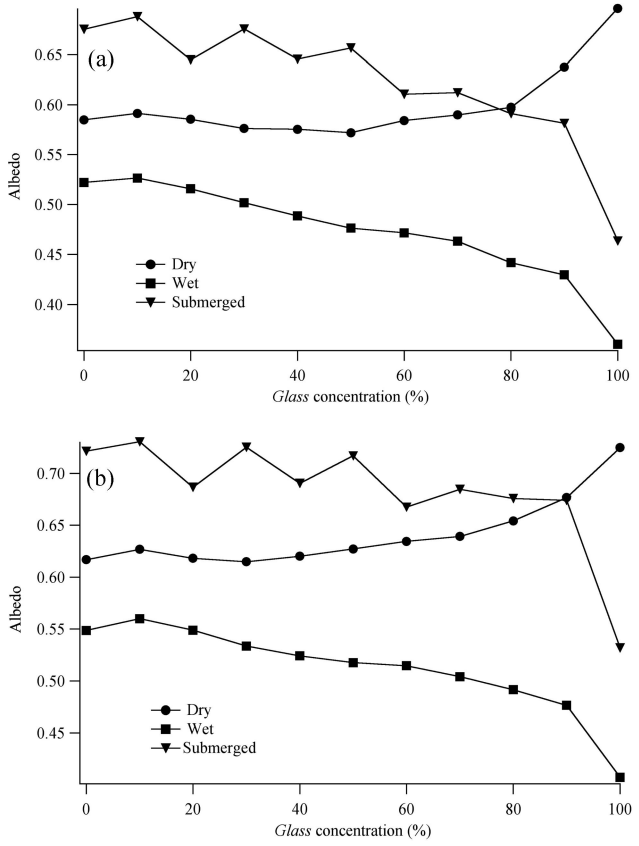

Fig. 5. Dry, water wetted, and submerged-in-water albedos of *Sample A–Glass* mixtures at (a) normal incidence and (b) 65° incidence.

(dry), 0.990 (wet), and 0.997 (submerged); for *Glass* the values are 0.998 (dry), 0.992 (wet), and 0.996 (submerged). Again, these values are derived from measured *REFF* values and the higher submerged values are discussed in Subsection 3.D.

Figure 6 shows $\alpha(60°)$ of the *Sample A–Glass* mixtures and the predictions made by Eq. (6). The areal prediction made by Eq. (1) is a simple linear relationship between the end points, does not fit well, and is not shown for clarity. It is seen that for dry and wet

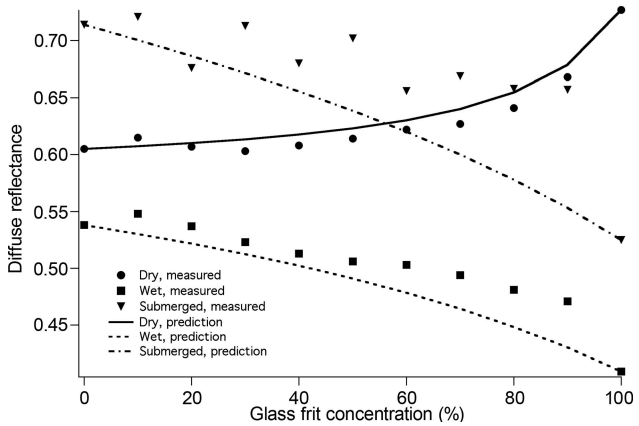

Fig. 6. Predictions of intimate mixture formula for diffuse reflectance (albedo at 60° incidence) of *Sample A–Glass* mixtures.

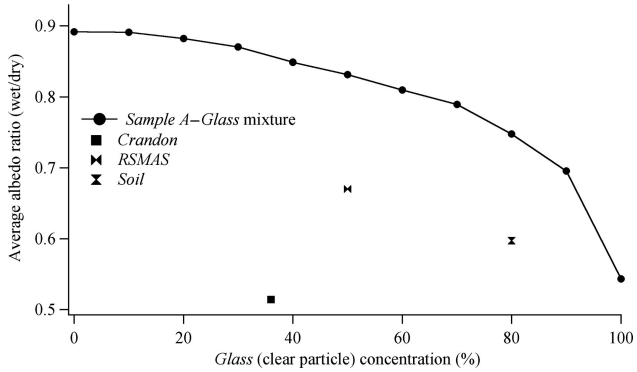

Fig. 7. Ratio of dry and wet albedos averaged over eight illumination angles versus translucent particle concentrations.

albedos, the intimate mixing formula fits the data within 3% and 10%, respectively. For submerged albedos, the measured data have large oscillations, and the 100% glass measurement is significantly different from the 90% value. Thus the mixing prediction cannot match this drastic change in albedo at higher glass concentrations.

It should be pointed out that, even if an accurate prediction of a mixture's albedo is available, such a prediction based solely on translucent particle concentration is unable to predict the wetting effect of the natural sand or soil samples used in this work. To illustrate this, we averaged the ratio of the wet and dry albedos over the eight illumination angles for the 11 concentrations of *Glass* and *Sample A*, and for *Crandon*, *RSMAS*, and *Soil*. These ratios are displayed versus the translucent particle concentrations in Fig. 7. One can see that the effect of wetting for the natural samples is much stronger than for the corresponding glass–ooid mixture. Part of this effect is probably because translucent particles in the natural samples are often colored. As mentioned in Subsection 3.B all the natural samples introduced in that subsection have more surface roughness present in the grains than does *Sample A*; as a rough surface would send some light obliquely enough to be totally reflected with a wetting liquid film, its surface should look darker than that of a smooth grain with the same other conditions. But the main point it shows is that to understand the mixtures one must have a good idea of the properties of the end members. Simply knowing the translucent particle concentration is not sufficient.

For totally opaque grains such as *Sample A*, our previous BRDF measurements[8] demonstrated that for both dry and wet layers only the top 2–3 mm layers would have an effect on the BRDF or albedo. For opaque particles, surface reflection by individual grains is predominant in the BRDF, and thus decreasing the refractive index contrast between the particles and the medium would not make the scattering penetrate significantly farther into the medium. However, this is not the case for layers containing translucent grains, since the decrease of the refractive index contrast would increase the forward scattering by the

translucent particles, and thus wetting-induced absorption enhancement should be much stronger.

D. Submerged Bidirectional Reflectance Distribution Function Measurements

We also investigated the effect of totally submerging the particles as opposed to simply wetting the surface. By totally submerging, we mean that the samples are measured completely underwater, with no water–air interface between the sample and the measuring device (the reflectance one would measure if diving in the water). If one goes back to the original LD and TBM models, submerged samples would not have an obvious interface (thus LD would predict no change). However, there would still be an increased forward scattering effect (TBM). So it is interesting to contrast the three cases: dry, wetted, and submerged. Most natural samples had a submerged effect that was between the wetted and the dry values, as shown in Fig. 3. However, *Sample A* had a submerged albedo at both normal and 65° incidence that was 16% higher than the corresponding dry albedo as shown in Fig. 2. This was verified with two more samples, another ooid sand from the Bahamas and a benthic sediment collected from Key Largo. This Key Largo sample was also an opaque shallow water sediment. To investigate this effect further we looked at the ooid–glass mixtures where we found that the submerged albedo decreased as the glass concentration increased (Fig. 5). The crossover of submerged and dry albedos occurs at approximately 80% glass concentration, where the submerged surface starts to become darker than the corresponding dry surface. It should be noted that the absolute REFF value of the sample depends on the REFF data of the calibration plaque.[9,11] Specifically, the REFF of a sample is obtained by taking the ratio of the radiance reflected from the sample to that from the Spectralon plaque and multiplying it by the REFF of the plaque. Our measurements of a submerged Spectralon plaque[11] also show that the REFF ($\theta_i = 0°$, $\theta_v < 55°$) is higher when the plaque is submerged than when dry.

E. Comparisons with Wetting Models

The results in Subsection 3.C show that a wetting prediction may not work well without taking into account factors such as the translucent particle concentration and particle surface roughness. Nevertheless, it would be informative to test how well the current models work when applied to various types of sediment. In Fig. 8 the wet albedo is plotted versus the corresponding dry albedo for the six natural sediments described above. The prediction by the TBM model with a dry asymmetry parameter of 0.7 and a wet asymmetry parameter of 0.9 is shown as the dashed curve (note that the TBM prediction made for 60° incidence is approximately 3% lower than for normal incidence where the dry albedo is between 0.3 and 0.7 and is much closer otherwise). The prediction made by the LD model with $n_{\text{particle}} = 1.6$ and $n_{\text{medium}} = 1.33$ is also shown in Fig. 8. These comparisons show that the shallow water sediments without

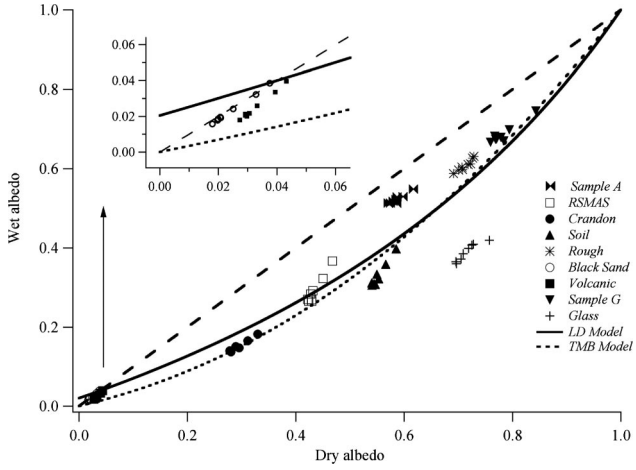

Fig. 8. Wetting predictions made by TBM and LD models with natural sediments. The long dashed straight line is dry = wet.

translucent particles have a smaller darkening effect than predicted by the models; for the other sediments, the *Crandon* and *RSMAS* sands agree well while *Soil* is less satisfactory. This demonstrates that a wetting model needs to incorporate translucent particle concentration as one of the input parameters.

It should be noted that the TBM theory is based on the assumption of isotropic multiple scattering, i.e., a particulate layer's REFF and albedo are given by[2]

$$\text{REFF} = \frac{\varpi^*}{4(\mu + \mu_0)} H(\mu)H(\mu_0), \tag{7}$$

where $\mu = \cos\theta_v$, and the albedo is approximated by

$$\alpha(\mu_0) = 1 - \sqrt{1 - \varpi^*}H(\mu_0), \tag{8}$$

where the H function is widely used in radiative transfers.[10,15] However, none of the dry REFF data in this work could be fitted to Eq. (7). Inferring a single-scattering albedo from the measured albedo [i.e., fitting to Eq. (8)] could also be unreliable, as all the information contained in the angular distribution of light is lost in the albedo data. Thus such a predictive attempt may only be tentative. Besides the isotropic

Table 1. Single-Scattering Albedo (SSALB) and Asymmetry Parameter ξ Values[a]

Index of Refraction	SSALB	ξ
$n = 1.6$, $k = 10^{-8}$	0.999981	0.7995
$n = 1.2$, $k = 10^{-8}$	0.999984	0.9305
$n = 1.6$, $k = 10^{-6}$	0.998184	0.8000
$n = 1.2$, $k = 10^{-6}$	0.998388	0.9307
$n = 1.6$, $k = 10^{-5}$	0.982443	0.8045
$n = 1.2$, $k = 10^{-5}$	0.984285	0.9321
$n = 1.6$, $k = 10^{-4}$	0.858256	0.8396
$n = 1.2$, $k = 10^{-4}$	0.867680	0.9434

[a]The data are derived from Mie scattering by spheres with a power-law size distribution with a mean radius of 100 μm and a variance of 0.1. The wavelength is 633 nm.

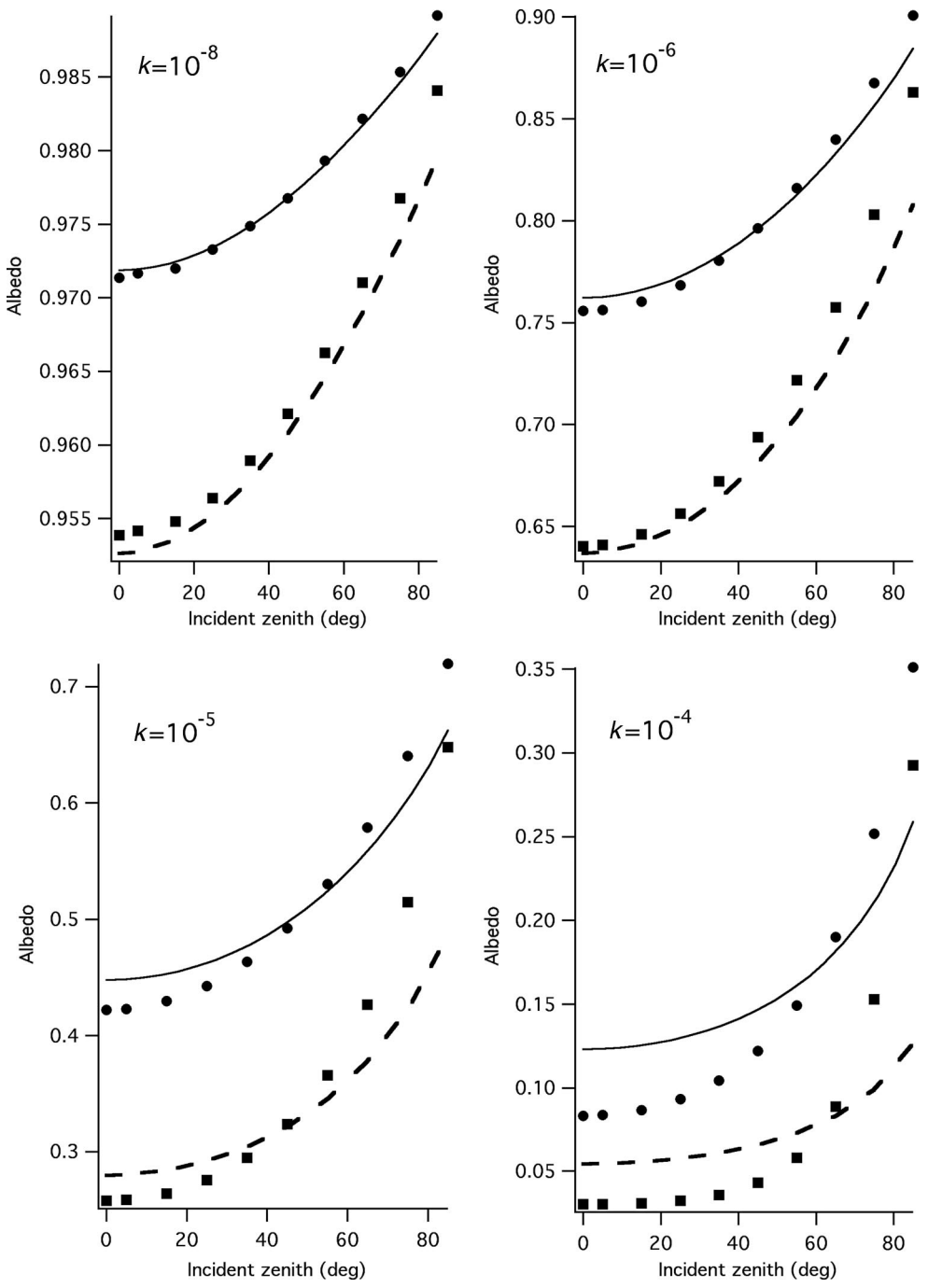

Fig. 9. Numerical check of the TBM model on hypothetical layers composed of spherical grains having a power-law size distribution with a mean radius of 100 μm and a variance of 0.1: ●, dry layer with refractive index $n = 1.6$; ■, wet layer with $n = 1.2$; solid curve, result of fitting albedos to the TBM model; dashed curve, the predicted values made by TBM. The imaginary refractive index k is indicated in each plot.

multiple-scattering assumption made in the TBM theory, another assumption made is that after wetting, the single-scattering albedo of the grains remains unchanged. This may be a rather accurate approximation for smooth particles (as shown below) but remains dubious for a rough particle. When a rough particle is coated by thin film, the effect of the thin film on the diffuse reflection could have a significant impact on its single-scattering albedo.

To further test the numerical accuracy of the TBM model, we performed radiative transfer calculations[16,17] on layers of dry and wet spherical particle layers. The hypothetical sample is a collection of spherical particles having a power-law size distribution[18] with a mean radius of 100 μm and a variance of 0.1. The real refractive index is assumed to be 1.6 when dry and 1.2 when wet (as assumed by the TBM model). The imaginary index is varied

from 10^{-8} to 10^{-4} and is not affected by the wetting process (note that natural particles are unlikely to have an imaginary refractive index much larger than 10^{-4} in the visible wavelength[19]). Table 1 is a summary of the single-scattering properties (Mie calculation results[16]), which shows that wetting smooth spherical particles causes few changes in the single-scattering albedo: here the biggest change in single-scattering albedo when going from dry to wet is less than 2% for $k = 10^{-4}$.

These single-scattering parameters together with phase functions are introduced into a radiative transfer code[17] to compute the directional albedo. The prediction procedure is outlined below with the example data for $k = 10^{-8}$ shown in parenthesis:

(1) Fit the dry albedo calculated by radiative transfer equation (RTE) versus the incident zenith to Eq. (8) to get a scaled single-scattering albedo ϖ^*(0.9999).

(2) With the known asymmetry parameter for dry particles (0.7995), use the inverse of Eq. (4) to convert ϖ^* to obtain the unscaled single-scattering albedo (0.99998).

(3) With the known asymmetry parameter for wet particles (0.9305), use Eq. (4) to obtain the scaled single-scattering albedo when wet (0.9997).

(4) Insert the scaled single-scattering albedo obtained from step (3) into Eq. (8) to get the predicted wet albedos, and compare with the RTE calculations made on $n = 1.2$.

Figure 9 shows that this prediction results in four representative k values from 10^{-8} to 10^{-4}. From Fig. 9 it is seen that, when absorption is low, the TBM prediction works well especially for near-normal illuminations. As the absorption increases, the albedo versus incident zenith becomes more anisotropic, and Eq. (8) does not fit well, thus causing inaccurate predictions for wet surfaces. This calculation was also run for two other size distributions of mean radii of 50 and 10 μm and similar results were obtained.

4. Conclusions and Suggestions

Through this series of measurements of wetted, submerged, and dry natural samples we have shown that the BRDF–REFF albedo depends on many factors, and the wetting effect cannot simply be described by either the LD or TBM models. Our measurements of the wetted REFF clearly show that, in some cases, we see enhanced forward scattering and reduced backscattering, evidence of the effect on which the TBM model is based. However, the results of the submerged measurements contrasted with the wetted results show that the air–water interface is also important, hence the LD model is also important. However, we have seen that an additional two parameters, which must also be considered in natural samples, can be very important: specifically, the fraction of translucent particles and the microscopic surface roughness of the individual particles. Specifically, the more translucent particles in a particulate layer, the brighter it is when dry, and the darker it is when wet. Thus the translucent particle concentration can be a large proportion of the wetting-induced darkening effect. The surface roughness of the particles is also important, as low albedo particles with a rough surface tend to have a larger wetting effect.

These results may have applications in remote sensing, as when a particulate surface is seen to have significant variation in reflectance between dry and wet, it is likely that such a surface contains translucent particles such as quartz sands. Furthermore, a quantitative model that can account for both the translucent particle concentrations and the individual grain surface roughness effects would be needed to make accurate predictions and inversions. Such a modeling effort might start with the current rough surface BRDF models [e.g., Ref. 20] that have both specular and diffuse reflection components, and by properly taking into consideration the increased forward scattering when wet, might give an accurate prediction of the wet BRDF and albedo.

We thank Arthur Gleason and Albert Chapin for help with the measurements and Michael Feinholz for providing the volcanic sand sample. This work was supported by the Office of Naval Research Ocean Optics Program.

References

1. C. F. Bohren, *Clouds in a Glass of Beer—Simple Experiments in Atmospheric Physics* (Wiley, 1987).
2. S. A. Twomey, C. F. Bohren, and J. L. Mergenthaler, "Reflectance and albedo differences between wet and dry surfaces," Appl. Opt. **25,** 431–437 (1986).
3. K. C. Jezek and G. Koh, "Effects of water and ice layers on the scattering properties of diffuse reflectors," Appl. Opt. **26,** 5143–5147 (1987).
4. G. Xu, M. Tazawa, P. Jin, and K. Yoshimura, "Diffuse reflection of ceramics coated with dielectric thin films," Appl. Opt. **42,** 1352–1359 (2003).
5. J. Lekner and M. C. Dorf, "Why some things are darker when wet," Appl. Opt. **27,** 1278–1280 (1988).
6. A. Angstrom, "The albedo of various surfaces of ground," Geogr. Ann. **7,** 323–342 (1925).
7. H. Zhang, K. J. Voss, R. P. Reid, and E. M. Louchard, "Bidirectional reflectance measurements of sediments in the vicinity of Lee Stocking Island, Bahamas," Limnol. Oceanogr. **48,** 380–389 (2003).
8. H. Zhang, K. J. Voss, and R. P. Reid, "Determining the influential depth of sediment particles by BRDF measurements," Opt. Express **11,** 2654–2665 (2003).
9. K. J. Voss, A. L. Chapin, M. Monti, and H. Zhang, "Instrument to measure the bidirectional reflectance distribution function of surfaces," Appl. Opt. **39,** 6197–6206 (2000).
10. B. Hapke, *Theory of Reflectance and Emittance Spectroscopy* (Cambridge U. Press 1993).
11. K. J. Voss and H. Zhang, "Bidirectional reflectance of dry and submerged Labsphere Spectralon plaque," Appl. Opt. **45,** 7924–7927 (2006).
12. M. U. Vera, P. A. Lemieux, and D. J. Durian, "Angular distri-

bution of diffusely backscattered light," J. Opt. Soc. Am. A **14,** 2800–2808 (1997).
13. C. F. Bohren, "Multiple scattering and some of its observable consequences," Am. J. Phys. **55,** 524–533 (1987).
14. A. Macke, M. I. Mishchenko, K. Muinonen, and B. E. Carlson, "Scattering of light by large nonspherical particles: ray-tracing approximation versus *T*-matrix method," Opt. Lett. **20,** 1934–1936 (1995).
15. B. Hapke, "Bidirectional reflectance spectroscopy 5: the coherent backscatter opposition effect and anisotropic scattering," Icarus **157,** 523–534 (2002).
16. M. I. Mishchenko, J. M. Dlugach, E. G. Yanovitskij, and N. T. Zakharova, "Bidirectional reflectance of flat, optically thick particulate layers: an efficient radiative transfer solution and applications to snow and soil surfaces," J. Quant. Spectrosc. Radiat. Transfer **63,** 409–432 (1999).
17. K. Stamnes, S. C. Tsay, W. Wiscombe, and K. Jayaweera, "Numerically stable algorithm for discrete-ordinate-method radiative transfer in multiple scattering and emitting layered media," Appl. Opt. **27,** 2502–2509 (1988).
18. M. I. Mishchenko, L. D. Travis, and A. A. Lacis, *Scattering, Absorption and Emissions by Small Particles* (Cambridge U. Press, 2002).
19. C. F. Bohren and D. R. Huffman, *Absorption and Scattering of Light by Small Particles* (Wiley, 1998).
20. B. van Ginneken, M. Stavridi, and J. J. Koenderink, "Diffuse and specular reflectance from rough surfaces," Appl. Opt. **37,** 130–138 (1998).